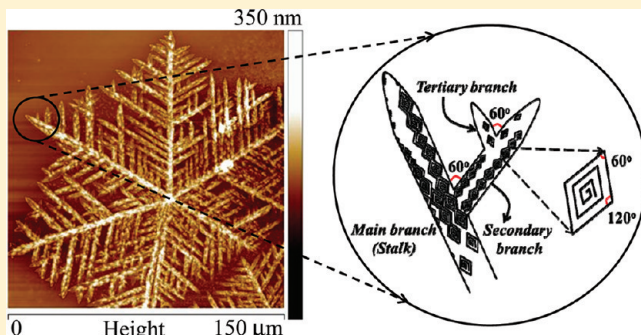


Phase-Separation-Induced Single-Crystal Morphology in Poly(L-lactic acid) Blended with Poly(1,4-butylene adipate) at Specific Composition

Siti Nurkhamidah and E. M. Woo*

Department of Chemical Engineering, National Cheng Kung University, Tainan, 701, Taiwan

ABSTRACT: The single-crystal morphology of poly(L-lactic acid) (PLLA) in blending with poly(butylene adipate) (PBA) in PLLA/PBA blends was for the first time reported in melt crystallization. At crystallization temperature (T_c) = 110 °C, by adding 30 wt % PBA into PLLA, the lamellae exhibit six-stalk dendrites with single-crystal packing. Phase separation and crystallization took place simultaneously at T_c = 110 °C in PLLA/PBA (70/30) blend, leading to discrete PBA domains and continuous PLLA domains. For PLLA/PBA (70/30) blend, all PBA were rejected from the growth front of PLLA crystals, expelled, and crystallized at ambient temperature as ring-banded PBA spherulites inside the discrete domains only, resulting in a favorable environment for formation of PLLA single crystals in the continuous domain. Atomic force microscopy (AFM) observation on individual crystallites reveals that lozenge-shaped single crystals were packed with a clockwise spiral pattern, stacked in 1–3 layers, and these lozenge-shaped crystals are aligned six hexasected directions into hexastalk dendrites with occasional side branches that are also aligned at 60° to main branches. The monolamellar thickness of lozenge-shaped single crystals was measured to be about 13–34 nm, and the dimension is about 0.8–3 μm along the short axis and 1.6–5 μm along the long axis. Typically, three layers of single crystals are stacked one on another; the lozenge crystals on the bottom layer are about twice as large as those on the top layer, forming a pyramid shape in the depth direction. Formation mechanisms of single crystals in melt-crystallized PLLA/PBA blend from 700 nm film thickness are discussed in correlation with exact phase separation at 30 wt % PBA.



1. INTRODUCTION

Conventionally, single crystals in polymers were most conveniently obtained from dilute solutions. Most poly(L-lactic acid) (PLLA) single crystals reported in the literature were solution grown from dilute solutions.^{1–6} Maillard and Prud'homme⁷ reported that PLLA single crystals can also be obtained by melt crystallization but from ultrathin film, ca. ~25 nm, at crystallization temperature (T_c) = 125 and 155 °C. Single crystals in neat PLLA by melt crystallization at T_c = 160 °C have also been reported by Kikkawa et al.; however, the thickness confinement in PLLA films had to be ultrathin at 100 nm or less.⁸ In those reported cases, two different shapes of PLLA single crystals were identified from either solution growth or melt crystallization: (1) hexagonal^{1–3,5–8} and (2) lozenge^{1–6} of mono- or multilayers. These PLLA single crystals are the same as or similar to the single-crystal shapes in poly(4-hydroxybutyrate) (PHB),⁹ poly(ϵ -caprolactone) (PCL),^{10–12} or poly(ethylene succinate) (PESu).¹³ The monolamellar layer of lozenge-shaped and hexagonal-shaped crystals has an average thickness of about 9–12 nm.^{2–6} For PLLA single crystals obtained from melt crystallization they have a monolayer hexagonal shape with a single-layer crystal thickness of 18 nm.^{7,8} The angles between growth faces of lozenge-shaped crystals are 60° and 120°.^{3,4,6} The crystal structure of PLLA single crystals from electron diffraction patterns is determined to be orthorhombic cell as the presence of two prominent (110) and (200)

diffraction peaks with very strong intensities, indicating highly ordered patterns in the single crystals.^{2,4,6,14} These two peaks and the crystal structure of PLLA single crystals are the same as that of PLLA in bulk samples with either α - or α' -form crystals.^{15,16} However, for bulk PLLA bulk samples (with randomly oriented crystal lamellae), usually not only (110) and (200) diffraction peaks but also (010) and (203) diffractions can be observed.^{15,16}

Block copolymers have been another common approach for examining the single-crystal behavior in PLLA. Some studies also demonstrate that PLLA single crystals can be obtained not only from neat PLLA homopolymer but also from either double crystalline–crystalline or crystalline–amorphous block copolymers, such as poly(L-lactide)-block-poly(ethylene glycol) (PLLA-*b*-PEG),¹⁷ poly(L-lactide)-*b*-poly(ethylene oxide) (PLLA-*b*-PEO),^{18,19} poly(L-lactide)-*b*-poly(methyl methacrylate) (PLLA-*b*-PMMA),²⁰ and poly(L-lactide)-*b*-polystyrene-*b*-poly(methyl methacrylate) (PLLA-*b*-PS-*b*-PMMA).²¹ PLLA single crystals from both PLLA-*b*-PEG and PLLA-*b*-PEO were obtained by melt crystallization of thin film which is prepared from dilute solution (0.1–1 wt %). For PLLA-*b*-PEG, single crystals of PLLA block

Received: June 29, 2011

Revised: September 23, 2011

Published: September 30, 2011

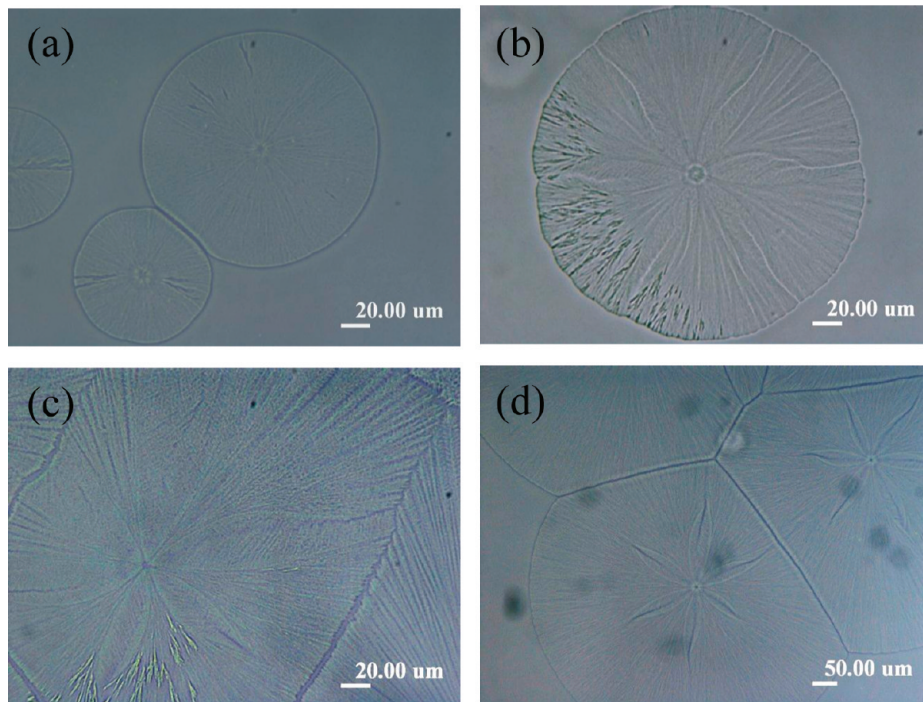


Figure 1. OM graphs for homogeneous PLLA/PBA blends melt crystallized at $T_c = 110\text{ }^\circ\text{C}$ at various compositions: (a) 100/0 (neat PLLA), (b) 90/10, (c) 80/20, and (d) 75/25. No phase-separation domains in these compositions.

and PEG block were obtained via a two-step crystallization. First, PLLA-*b*-PEG crystallized at 120 °C to crystallize PLLA block and PEG block is in the melt state resulting in single crystals with different kinds of shape: lozenge-spiral growth, lozenge multilayer, and hexagonal multilayer with a monolamellar thickness of about 12–14 nm. Then, the sample is quenched to 35 °C to crystallize PEG block, and the morphology of PEG block is layer dendritic crystals formed at the edge of PLLA single crystals. Yang et al.¹⁷ suggested that there are two possible reasons why PLLA block can form single crystals in PLLA-*b*-PEG from melt crystallization: (1) PLLA block and PEG block are miscible in the melt state, and PEG block may play a dilute solvent that provides a favorable environment where PLLA block may assume macroconformations and both PLLA and PEG blocks are separated from each other before crystallization, (2) PLLA block has a lower molecular weight average ($M_w = 5000\text{ g/mol}$); thus, the entanglement degree of the molecular chain is very low, which is advantageous for the molecules to fold and form single crystals.

In addition, Huang et al.¹⁸ investigated the crystallization behavior of PLLA-*b*-PEO with two different molecular weights of PLLA block. The result shows that PLLA single crystals can be formed in PLLA-*b*-PEO only at certain conditions: (1) low M_w of PLLA block, (2) ultrathin film (80–100 nm), and (3) $T_c = 110$ and 120 °C. Recently, Huang et al.¹⁹ investigated further the dependence of crystalline morphology on T_c and film thickness of PLLA-*b*-PEO with low M_w of PLLA block. A hexagonal dendrite stacked with PLLA single crystals has been observed in PLLA-*b*-PEO copolymer thin films (220 nm). The interplay of crystallization of PLLA block, microphase separation between two blocks, and the effect of diffusion limitation in thin films have been suggested as the possible reason for formation of PLLA single crystals. Formation of alternating crystalline and amorphous layers driven by crystallization of PLLA and microphase separation is attributed to formation of PLLA single crystal in

PLLA-*b*-PEO.¹⁹ In addition to PLLA block copolymers, there are several other block copolymers exhibiting single-crystal morphology, i.e., PEG-*b*-PCL¹² and polystyrene-*b*-poly(ethylene oxide) (PS-*b*-PEO).²² PEG-*b*-PCL, which is prepared by solution-grown single crystals, exhibits an elongated hexagonal shape. The single-crystal shape of PEG-*b*-PCL is different from the two homopolymers, PEG and PCL. The geometry of PEG single crystals is square,^{12,23} whereas that of PCL single crystals exhibits a hexagon shape.^{10–12} In those studies the authors suggest that such results are caused by the double effects of microphase separation and crystallization of two crystalline PEG and PCL blocks.¹²

Controlled blending of PLLA with other polymers has been relatively less attempted in studying the single-crystal behavior. For other polyesters, such approaches have been preliminarily proven to be promising as long as the phase behavior in the blend is properly utilized to achieve ideal conditions for formation of single crystals. The single-crystal morphology has also been observed in the blend system of PESu/tannic acid (TA) blend.²⁴ Lozenge-shaped crystals packing into seaweed-like dendritic crystals are the crystalline morphology of PESu/TA (80/20) blend. The authors suggest that such single-crystal-like dendrites are induced by the strong hydrogen-bonding interactions between PESu and TA in the melt crystallization.²⁴ Lozenge-shaped crystals from melt crystallization in PESu/TA blend are equivalent to those from solution-grown single crystals in neat PESu¹³ with a monolamellar thickness of 7–8 nm.^{13,24} In a previous study, the single-crystal morphology of PLLA was observed only in neat PLLA and PLLA block copolymers from dilute solution or ultrathin film. For the first time, the single-crystal morphology of PLLA in phase-separated blends of two semicrystalline homopolymers by melt crystallization of intermediate thin films (700 nm to micrometer thickness) was discovered, analyzed, and reported. The behavior of single crystals in PLLA

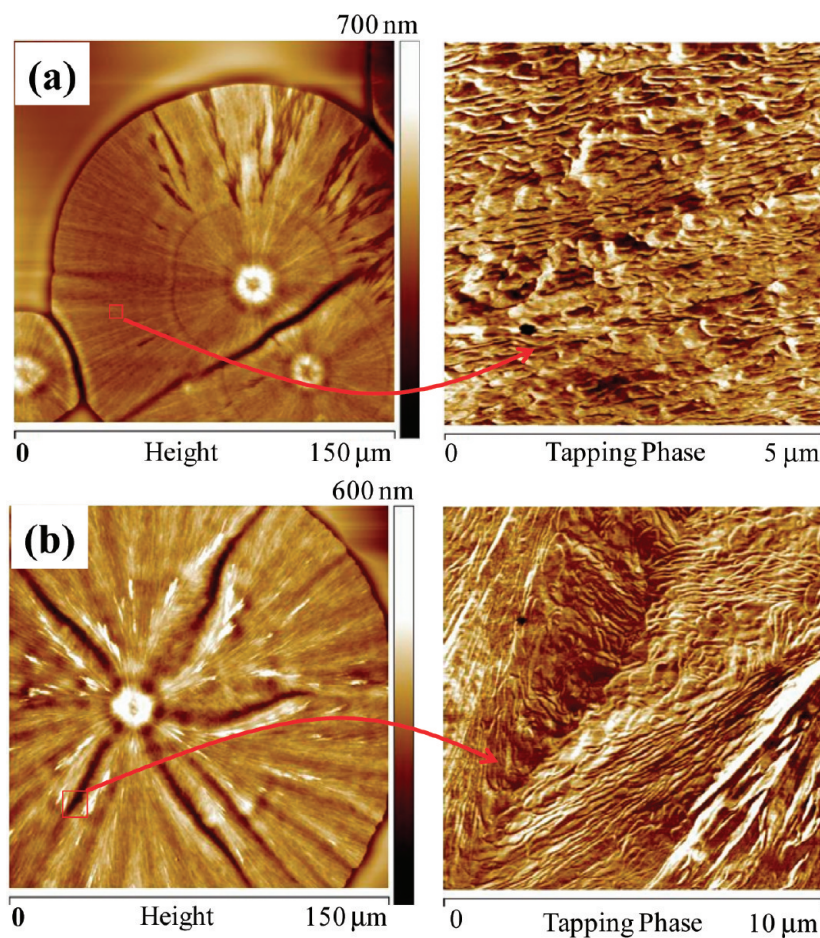


Figure 2. AFM height (left column) and phase images (right column) of (a) neat PLLA and (b) PLLA/PBA blend (90/10) crystallized at 110 °C.

blends initiated in phase separation would constitute an interesting comparison to earlier block copolymer systems.

2. EXPERIMENTAL SECTION

2.1. Materials and Preparation. Poly(L-lactic acid) (PLLA) was purchased from Polysciences, Inc. (Warrington, PA) with a relatively low weight-average molecular weight (M_w). The PLLA polymer was characterized in house using gel permeation chromatography (GPC, Waters) to reveal $M_w = 11\,000$ g/mol (PDI = 1.1). For this grade of PLLA, the glass transition temperature (T_g) = 45.3 °C and melt temperature (T_m) = 155 °C. Poly(1,4-butylen adipate) (PBA) was purchased from Aldrich (St. Louis, MO) with a weight-average molecular weight of 12 000 g/mol, PDI = 1.30, $T_g = -68$ °C, $T_m = 54$ °C, and degradation temperature (T_d) = 250 °C.

Thin film samples (700 nm) of PLLA/PBA blends were prepared by spin coating a solution of PLLA/PBA dissolved in chloroform at a concentration of 4 wt % onto glass slides using a spin coater (Chemate Technology Spin-Coater KW-4A, Northridge, CA) at 3500 rpm for 40 s. Samples were heated on a hot stage to a maximum melting temperature ($T_{max} = 190$ °C) for 10 min for erasing prior crystals and then rapidly removed to another hot stage preset at a designated isothermal $T_c = 110$ °C.

2.2. Apparatus and Procedures. Polarized optical microscopy (POM, Nikon Optiphot-2, Tokyo, Japan), equipped with a digital camera charge-coupled device (CCD) and a microscopic

hot stage (Linkam THMS-600, Surrey, U.K.) with a TP-92 temperature programmer, was used for characterizing the crystalline morphology.

Atomic force microscopy (AFM, *diCaliber*, Veeco Corp., Santa Barbara, CA) investigations were made in intermittent tapping mode with a silicon tip ($f_0 = 70$ kHz, $r = 10$ nm) installed. Thin films were deposited on substrates of glass slides with an open face for AFM characterization. AFM measurements were also used to measure the sample and monolamellar thickness in PLLA/PBA blends.

3. RESULTS AND DISCUSSION

Neat PLLA and PLLA/PBA blends of (90/10) to (75/25) compositions are homogeneous without phase domains at high temperatures above T_m 's of both constituents or upon cooling to crystallize. The PLLA crystals in these blend compositions remained well-rounded spherulites without dendritic patterns. Figure 1 shows OM for (a) neat PLLA, PLLA/PBA blends of (b) 90/10, (c) 80/20, and (d) 75/25 at $T_c = 110$ °C. No phase-separation domains were observed either at T_c or upon cooling the PLLA/PBA blends (90/10 to 75/25) to ambient temperature. For these compositions, PBA at T_c was a molten diluent to crystallizing PLLA. However, the blends were homogeneous without phase-separation domains. Other than some of the lamellae in spherulites appearing fluffy, no single crystals resulted in these compositions.

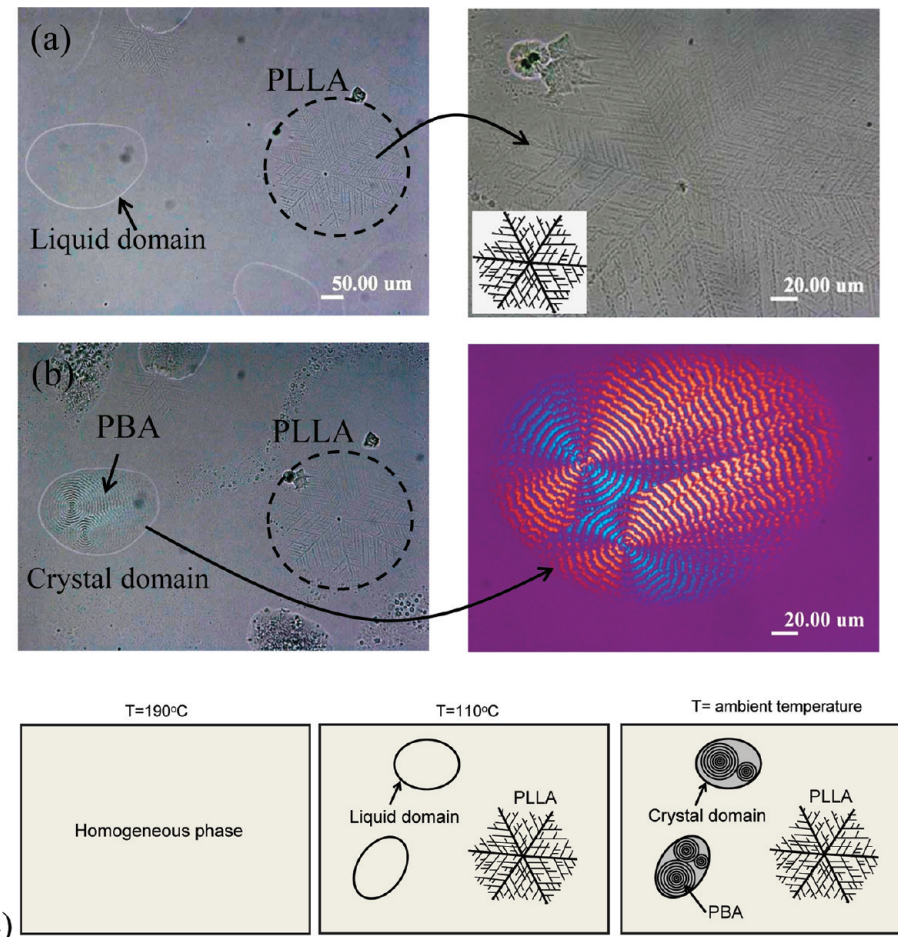


Figure 3. OM and POM micrographs for PLLA/PBA (70/30) blend crystallized at $T_c = 110\text{ }^\circ\text{C}$: (a) only PLLA dendrites when held at T_c , (b) PBA ring-banded spherulites and PLLA dendrites when cooled to ambient temperature for 4 min, and (c) scheme for POM morphology of blend held at $T = 190\text{ }^\circ\text{C}$, $110\text{ }^\circ\text{C}$, and ambient temperature ($28\text{--}30\text{ }^\circ\text{C}$).

Details of the surface morphology of spin-coated PLLA/PBA blends of various compositions fully crystallized at a specific T_c (then cooled to ambient temperature) were characterized using AFM. AFM characterization on the T_c -crystallized ($110\text{ }^\circ\text{C}$) and ambient temperature-cooled (at $28\text{--}30\text{ }^\circ\text{C}$) PLLA/PBA samples was focused on the PLLA crystal patterns. Figure 2 shows AFM height images of (a) neat PLLA and (b) PLLA/PBA blend (90/10) crystallized at $110\text{ }^\circ\text{C}$. Zoomed-in images of the square box in AFM phase images are shown to reveal greater details of surface morphology. In general, PLLA crystals in PLLA/PBA (100/0) and (90/10) blends are arranged by edge-on lamellae, and no single-crystalline morphology of PLLA can be observed in neat PLLA or PLLA-rich blend compositions, where no phase separation takes place. AFM height images for various blend compositions (all crystallized at the same $T_c = 110\text{ }^\circ\text{C}$) show that the morphological patterns of PLLA crystals vary significantly with respect to the blend composition. For PLLA/PBA 90/10 blend, there are no visible changes in the spherulite patterns (as viewed in POM graphs, not shown here for brevity) between $T_c = 110\text{ }^\circ\text{C}$ and cooling to ambient temperature ($29\text{--}30\text{ }^\circ\text{C}$). For PLLA/PBA (90/10) blend, the PBA component is crystallized and trapped inside the PLLA spherulites and due to PBA is only in a small amount (10 wt % in blends), the later crystallization of PBA at ambient temperature does not cause any significant changes in the precrystallized PLLA crystals.

As the PBA content in the PLLA/PBA blend reached 30 wt % or above, phase separation took place upon cooling from the molten state at T_{\max} to $T_c = 110\text{ }^\circ\text{C}$ to crystallize, and both phase domains and crystals were vividly present in PLLA/PBA (70/30) blend. As shown in the previous figures, there is no phase separation when the contents of PBA in PLLA/PBA mixtures are less than 30 wt %. Preliminary POM characterization was performed on the crystal patterns in PLLA/PBA (70/30) crystallized at $T_c = 110\text{ }^\circ\text{C}$ and then cooled to ambient temperature. When held at $T_c = 110\text{ }^\circ\text{C}$, only the PLLA component in the PLLA/PBA blends would crystallize but PBA did not crystallized at $T_c = 110\text{ }^\circ\text{C}$. Because the T_m of PBA is much lower than the T_c , the morphology of PLLA/PBA blends at T_c belongs to PLLA crystals and PBA crystallizes only at ambient temperature. The phase domains were visible using POM or OM characterization in PLLA/PBA (70/30) blend, which was used as an illustration for such phase-separation and crystal morphology. Figure 3a and 3b shows *in situ* POM monitoring on growth of PBA crystals upon cooling to ambient temperature at $29\text{ }^\circ\text{C}$ for time $t = 0\text{--}4$ min in the PLLA/PBA (70/30) blend system following melt crystallization of PLLA at $110\text{ }^\circ\text{C}$. Inset graphs show enlargements of the PLLA single-crystal dendrites grown in the hexagonal peripheral and PBA phase domains, respectively, of two specific spots. For better visualization, the scheme in Figure 3c summarizes the main features of the POM morphology for

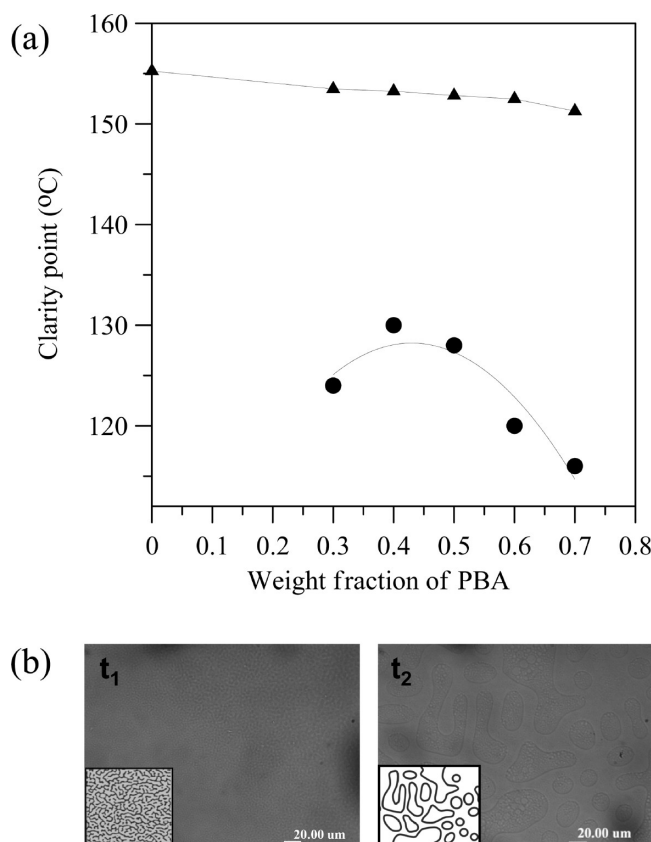


Figure 4. (a) UCST phase diagram with clarity points for PLLA/PBA blends as a function of composition. (b) Size of phase-separated domains as a function of time ($t_2 - t_1 < 10\text{s}$) for PLLA/PBA (70/30).

PLLA/PBA (70/30) blend upon being kept at temperature (T) = 190 °C (one-phase homogeneous liquid mixture), then held at 110 °C (dendritic PLLA crystal being crystallized), and finally cooled to ambient temperature (29–30 °C), where the PBA component in the blend is crystallized into ring-banded spherulites in discrete phase domains.

In the OM graphs for PLLA single crystals, it appears that all individual branches and side branches of the dendritic single crystals grow at a 60° angle to each other. Coincidentally, the 60° angle is exactly the same angle between the six main lamellar stalks, which radiate out from common nuclei eye and equally divide the dendrites into six evenly divided portions. The mechanism of crystal growth along the 60° angle is a result of the basal angle of the single crystals, which will be discussed further in the following AFM analysis of larger magnifications and clearer images. At T_c , only PLLA crystallizes as dendritic single crystals, as indicated by the circle dashed line in the graphs. In addition to the PLLA dendrites, liquid-phase domains appear upon being held at T_c , and apparently at this T_c , the interior of the phase domains is filled with only molten polymers in the melt state (showing no optical birefringence). However, the PBA component solidifies and crystallizes as ring-banded spherulites inside the phase domains upon cooling down and holding at ambient temperature (~28–30 °C), appearing as PBA ring-banded spherulites surrounded by phase domains with an average size of ~150–200 μm. After 30 s at ambient temperature, there were two small ring-banded spherulites of PBA crystals. With a further increase of time at ambient temperature

up to 4 min, the PBA ring-banded spherulites were completely crystallized to fill in the whole phase domain as shown in Figure 3b.

For PLLA/PBA (70/30) blend, there are apparent phase domains appearing at T_c and PBA crystallizes as ring-banded spherulites in the domains upon cooling from T_c to ambient temperature. The phase behavior in PLLA/PBA blends was characterized using POM with regular film thickness (~10 μm), and the result showed that this blend system exhibited upper critical solution temperature (UCST) behavior below the melting temperature of PLLA. Figure 4a shows the UCST phase diagram for PLLA/PBA blend, which indicates that this blend system is homogeneous above UCST (close to PLLA T_m), but cooling to below UCST for crystallization would induce phase separation in the PLLA/PBA blend. As shown in the figure, UCST behavior only occurs at certain compositions and temperatures. This phenomenon can be explained thermodynamically. For a mixture (blend) composition to be stable, there are two criteria that must be fulfilled: (1) the value of the Gibbs free energy of mixing must be smaller than zero (negative), and (2) the second-order partial derivatives of the Gibbs free energy of mixing with respect to the composition of component i at constant temperature and pressure must be larger than zero. However, for a certain composition of mixture there might be a local maximum value of the Gibbs free energy of mixing present in the blend systems. At this composition, phase separation is present in the blend systems.²⁵ There are two major mechanisms of phase separation: spinodal decomposition and nucleation–growth. For the nucleation–growth mechanism, the size of the phase-separated domain increases with time.²⁶ As can be seen in Figure 4b, with increasing time the size of the phase-separated domain increases. This result shows that for the PLLA/PBA (70/30) blend composition crystallized at 110 °C it is clearly due to the nucleation–growth mechanism instead of the spinodal decomposition one.

To prove that the ring-banded spherulites in the phase domain are PBA crystals, a fully crystallized PLLA/PBA (70/30) blend sample was heated from ambient temperature to 55 °C (above the T_m of PBA). Figure 5 shows PLLA in the phase-separated PLLA/PBA (70/30) blend melt crystallized at 110 °C and then cooled to (a) ambient temperature and then heated to (b) T = 55 °C to melt PBA. Morphology evolution of the crystallized and phase-separated blend upon heating indicates clearly that the discrete domains are mainly populated by PBA, where the PBA ring-banded spherulites in the discrete domains completely disappeared but PLLA dendrites remained intact up to melting point of ~157 °C. After being heated to 55 at 2 °C/min, the ring-banded spherulites in the phase domains melt and no longer exist. By contrast, the dendritic single crystals remain the same at 55 °C, as indicated by the circle dashed line in Figure 5b, but they completely melt at a temperature of ~157 °C (graph not shown here). On the basis of this result and the melting temperature of PLLA and PBA, the dendritic single crystals and circular ring-banded spherulites in PLLA/PBA (70/30) blend can be identified as the PLLA and PBA crystals, respectively. It should be noted that with a further increase of temperature up to 240 °C all crystals in the blend sample completely melted and only amorphous phase domains were visible in OM. After being cooled to ambient temperature, ring-banded PBA spherulites reappeared inside the phase domains. Apparently, the PBA component was rejected to discrete domains and only crystallized inside the

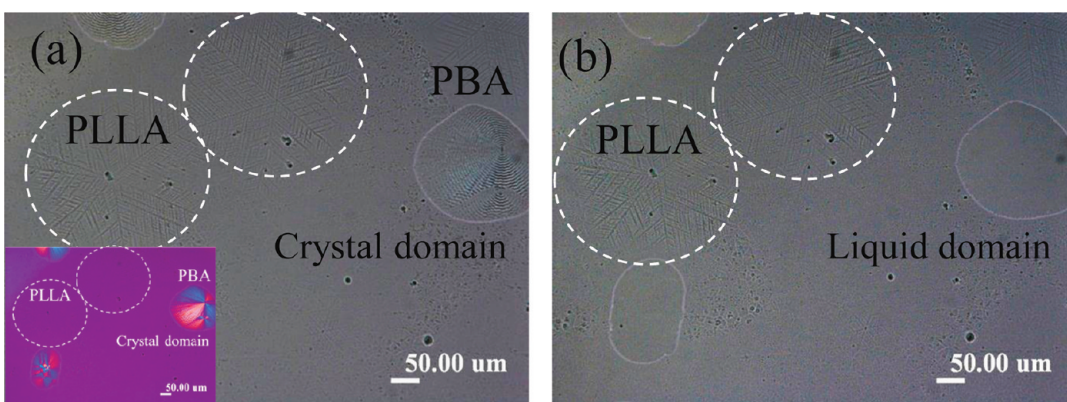


Figure 5. Dendritic PLLA crystal in phase-separated PLLA/PBA (70/30) blend melt crystallized at 110 °C and then cooled to (a) ambient temperature and then heated to (b) $T = 55$ °C to melt the PBA crystals.

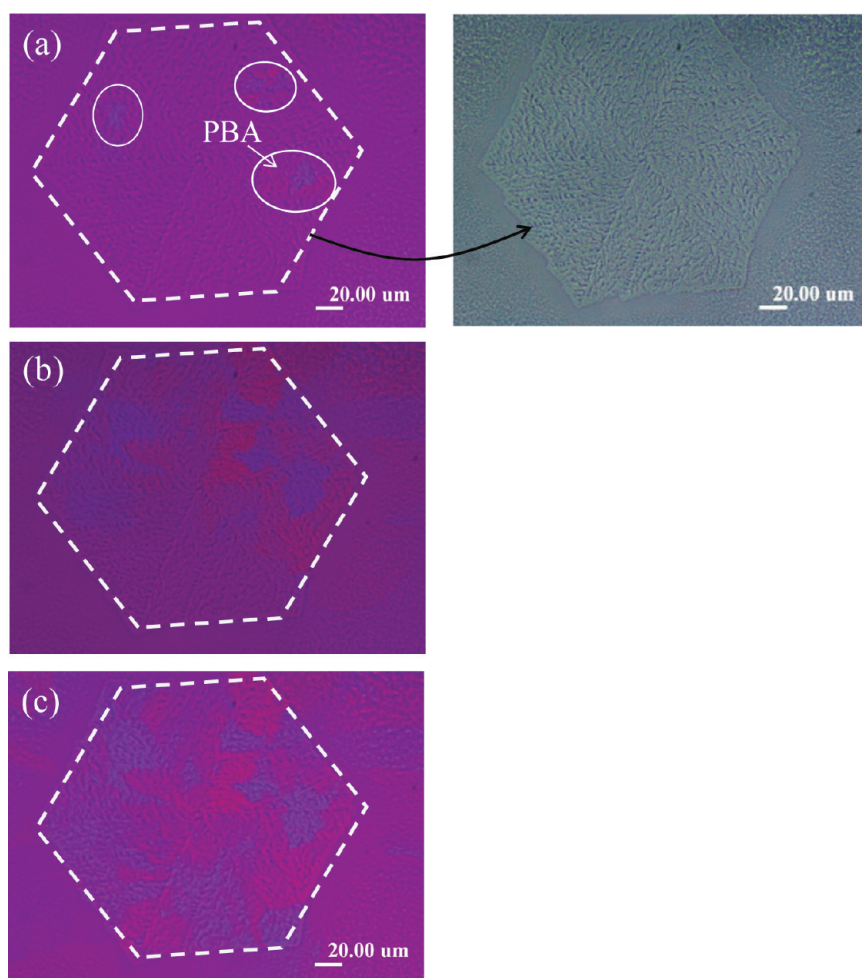


Figure 6. POM and OM micrographs showing time-dependent secondary growth of PBA on top of precrystallized PLLA hexagon crystals of PLLA/PBA (50/50) blend upon cooling from $T_c = 110$ °C to ambient temperature. Time held at ambient temperature (28–30 °C): $t =$ (a) 20, (b) 120, and (c) 240 s.

discontinuous phase domains; PLLA only crystallized at T_c in the continuous domain.

Maillard and Prud'homme⁷ reported that the chain axis of single crystals is oriented normal to the substrate. This means that the lamellar chains of PLLA single crystals are perpendicular

to the plane of the sample, resulting in PLLA dendritic single crystals without birefringence when they are observed using POM. The other possibility of why there is no birefringence in PLLA crystal is due to the lamellar thickness of it compared to film thickness. The thickness of samples is about 700 nm;

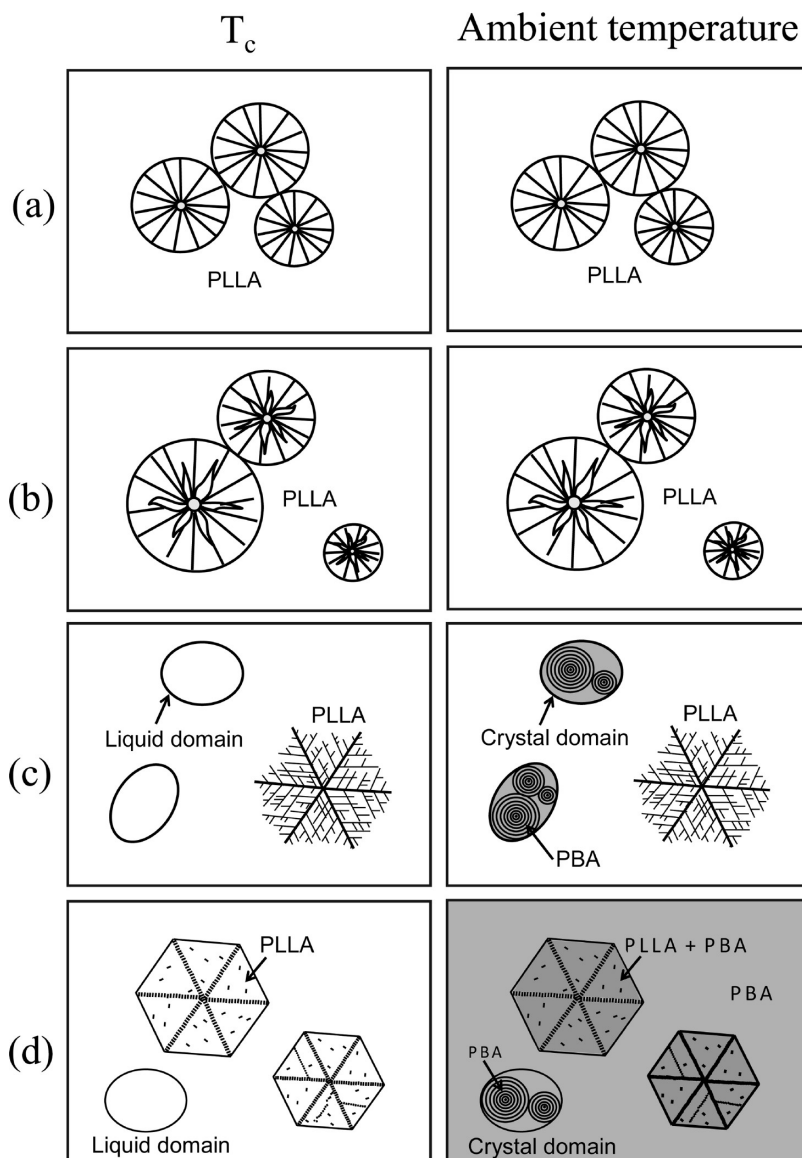


Figure 7. Schematic diagrams showing morphology transformation in (a) neat PLLA and PLLA/PBA blends crystallized at 110 °C for compositions (b) 90/10, (c) 70/30, and (d) (50/50).

however, the thickness of the regions in which the dendritic single crystals form is about 90 nm (measured by AFM). With the thin thickness (700 nm), the dendrites or single crystals are thin enough and flat enough to cause no significant birefringence across the lamellae width or length.

There are phase-separated domains appearing at $T_c = 110$ °C not only in PLLA/PBA (70/30) but also in PLLA/PBA (50/50) blend. However, the number of domains in the PLLA/PBA (70/30) blend is more than that in the PLLA/PBA (50/50) blend. PLLA crystallizes in hexagonal dendrites for PLLA/PBA (50/50), and there is no birefringence at T_c the same as the dendritic single crystals of PLLA in PLLA/PBA (70/30). Figure 6 shows that upon cooling to ambient temperature the abundant PBA component crystallizes not only inside the discrete PBA domains but also in the whole area of PLLA hexagon crystals. The discussion here is focused on the morphology of PLLA instead of discrete domains. Hexagonal-shaped PLLA crystals, owing to the thin thickness and low crystal birefringence in POM, could be

identified clearly only using either OM or AFM microscopy. However, POM microscopy was used instead of OM or AFM to clearly illustrate not the PLLA hexagon crystals but the PBA spherulites. The later crystallization of PBA in the blend at ambient temperature does not change the spherulites patterns of PLLA originally set at $T_c = 110$ °C; rather the PBA crystallization on PLLA only enhances the birefringence of the originally low-birefringence hexagonal dendrites of PLLA. Figure 6a shows that PBA crystallizes on top of the hexagonal dendrites of PLLA after being kept at ambient temperature for 20 s, as marked by circle inside the hexagonal crystals. The inset graph is the OM micrograph of Figure 6a showing hexagonal crystals of PLLA. At $t = 120$ s at ambient temperature of 29–30 °C, the PBA component crystallizes almost to spread all over the whole area of PLLA hexagonal crystals. With a further increase of time at ambient temperature up to 240 s, PBA has already not only crystallized within the hexagonal dendrite of PLLA but also extended to outside of hexagonal crystals, as observed in Figure 6c.

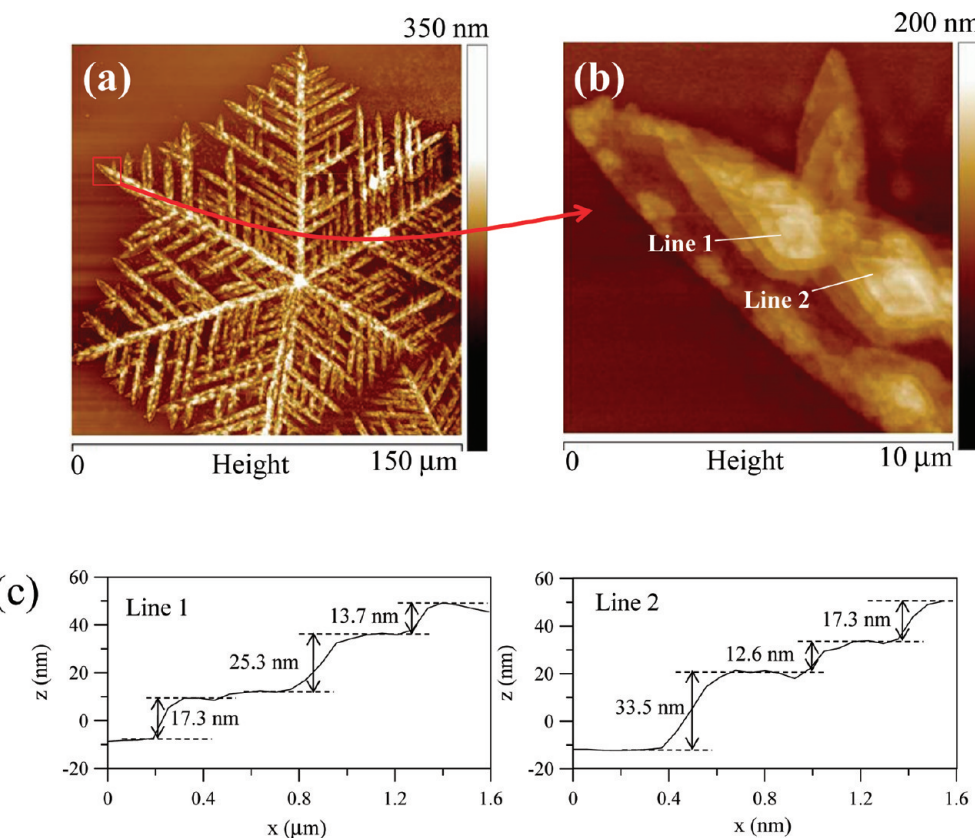


Figure 8. AFM images of dendritic single crystals in PLLA/PBA (70/30) blends crystallized at 110 °C: (a) height image, (b) zoom-in of the square-box shown in the right side of graph a, and (c) height profiles of lines 1 and 2 in graph b.

The PBA component in the blend crystallizes at ambient temperature of ~29 °C as ring-banded spherulites inside the PBA discrete domains, whereas the pattern or morphology of PBA crystallizes outside the domains cannot be observed clearly owing to low birefringence.

The morphology of PLLA crystals and final dendrite patterns could be controlled by phase separation and domains with addition of various weight fractions of PBA in PLLA/PBA blends. Single crystals with lozenge-shaped pyramidal packing appear to occur only at the specific composition of PLLA/PBA (70/30). Figure 7 shows schematic diagrams of the 110 °C crystallized morphology evolution of PLLA/PBA blends of different PBA content: (a) 100/0, (b) 90/10, (c) 70/30, and (d) 50/50, each of the blends being stepwise crystallized at T_c (left column) and then cooled to ambient temperature (right column). At $T_c = 110$ °C, neat PLLA exhibits well-rounded Maltese-cross spherulites with no dendrites. By adding 10–25 wt % PBA in blend, the PLLA/PBA/(90/10) blend crystallized at $T_c = 110$ °C exhibits similarly well-rounded spherulites but some lamellae start to twist to exhibit a flower-like pattern in the center of the spherulites with increasing PBA contents in the blends. At 10–25 wt % PBA blends the PLLA/PBA blends are homogeneous without phase domains, and no single crystals of PLLA are observed when crystallized at $T_c = 110$ °C; however, with addition of 30 wt % of PBA in PLLA/PBA blends, the phase-separated PLLA/PBA (70/30) blend can exhibit single-crystalline dendrites when crystallized at $T_c = 110$ °C, indicating dramatic effects of blending composition and phase separation on PLLA crystalline morphology. Both PLLA/PBA (70/30) and

(50/50) blends exhibit phase separation; however, phase domains are different. As a result, the hexagonal dendrites in PLLA/PBA (50/50) blend are not packed by single crystals as observed in AFM images (not shown here for brevity) for PLLA/PBA (70/30) blend. Because PBA in PLLA/PBA (50/50) not only crystallizes inside the PLLA domains like it does in PLLA/PBA (70/30) blend but also extends outside the PLLA domains, the number of domains in PLLA/PBA (50/50) blend is fewer than that in the PLLA/PBA (70/30) blend. The gray-color schemes (right column) in Figure 7d for OM morphology taken at ambient temperature for the samples indicates that PBA crystallizing at this temperature enhances the birefringence in the entire domains of the sample. It means that even though there are phase domains in PLLA/PBA (50/50), some of excess molten/liquid PBA is expelled and present in the growth front of PLLA crystals, which hinders formation of PLLA single crystals like the one seen in PLLA/PBA (70/30) blend.

Note also here that this study showed that other PLLA/PBA blend concentrations (other than 70/30) led to a variety of crystal/spherulite morphology but not dendrites with lozenge single crystals. Blends with lower PBA contents (<30 wt %) led to well-rounded PLLA spherulites. Other compositions such as PLLA/PBA (50/50), though showing similar phase domains as the PLLA/PBA (70/30), exhibited a PLLA morphology of hexagonal dendritic spherulites but not packed by single crystals as viewed using AFM. Thus, the focus in this study was placed on the PLLA/PBA (70/30) blend composition exhibiting lozenge single crystals induced by the particular phase separation. The following

discussion is focused on the dendritic PLLA single crystals of lozenge shape found in the PLLA/PBA (70/30) blend.

The PBA component ($T_m = \sim 54^\circ\text{C}$) in the PLLA/PBA (70/30) blend was in molten liquid domains at $T_c = 110^\circ\text{C}$ and then crystallized only inside the discrete domain as small ring-banded spherulites at ambient temperature, and the region outside the discrete PBA phase domain is a continuous phase and mainly composed of PLLA component, which crystallized into dendritic single crystals at $T_c = 110^\circ\text{C}$ and remained the same dendritic pattern at ambient temperature. In this continuous phase region, only PLLA crystallized at $T_c = 110^\circ\text{C}$; PBA component in the continuous phase was so poor that it did not crystallize and acted only as an amorphous diluent to PLLA's crystallization in initiating the dendritic lamellae with single-crystal packing. The individual lozenge-shaped crystals packed in the dendritic branches were then further analyzed using AFM height and phase imaging, to be discussed in the following.

Lozenge-Shaped Single Crystals in Phase-Separated Blend. As discussed, the composition effects on the PLLA crystals are apparent as the blends of various compositions are approaching a single-crystalline pattern at a PBA content being at or near 30 wt %. The greater amount of PBA in PLLA/PBA blend (70/30) is responsible for PLLA being able to pack into dendritic single crystals when melt crystallized at $T_c = 110^\circ\text{C}$. Note that this unique single-crystal pattern was not observed at all in neat PLLA (unblended with PBA) when melt crystallized at any T_c . Neat PLLA has been reported to exhibit single crystals only when it is solution crystallized from dilute solutions^{1–6} or melt crystallized from ultrathin film.^{7,8} By contrast, in the PLLA/PBA (70/30) blend investigated, melt crystallization in thin films of 700 nm is shown to easily pack into single crystals of lozenge shapes.

As discussed earlier, PLLA in PLLA/PBA (70/30) blend has an interesting morphology appearing as dendritic single crystals when viewed in POM, which was capable of revealing the entire dendritic branches of the single-crystal packing. Greater magnification by AFM was needed for better morphological details of individual crystal species in the minute branches. Figure 8 shows AFM images of dendritic single crystals in PLLA/PBA (70/30) blends crystallized at 110 °C: (a) height image, (b) zoom-in of the square-box shown on the right side of graph a, and (c) height profiles of lines 1 and 2 in graph b. Individual single crystals with lenticular shapes 4–5 μm in long length or 2–3 μm in short length became very clear in AFM images. The main and side branches of dendrites are arranged by lozenge crystals as shown in Figure 8b. Lozenge-shaped single crystals with spiral growth can be observed clearly in the main branch (Figure 8b). Height profiles along lines 1 and 2 as marked on the graphs are shown below in Figure 8c. The height profiles along lines 1 and 2 show clearly that the thickness of each layer of lamellae of lozenge-shaped single crystals is about 13–34 nm, depending on layer locations.

It has been reported that the thickness of monolamellar PLLA single crystals which are obtained by solution-grown crystals and melt crystallization are 9–12^{2–6} and 18 nm,⁷ respectively. Thus, the average thickness of monolamellar of PLLA single crystals in melt-crystallized PLLA/PBA (70/30) blend is about the same magnitude of that of homopolymer single crystals prepared from solution-grown crystal and melt crystallization, respectively. The other known ways to obtain dendritic single crystals of PLLA were by crystallizing the polymers in confinement of ultra-thin films (less than 30 nm of thickness).⁷ In this study, the film

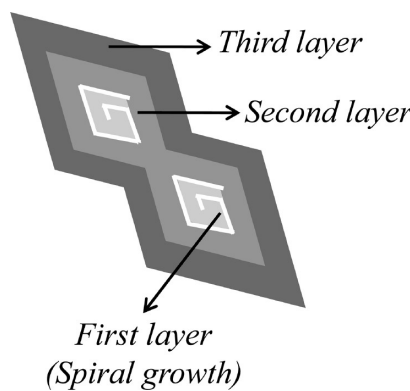


Figure 9. Scheme of single-crystal layers in branches or stalks of dendrites of PLLA/PBA (70/30) blend crystallized at $T_c = 110^\circ\text{C}$.

thickness (about 700 nm) of the PLLA/PBA blends does not have to be very ultrathin, which is 23 times thicker than the ultrathin films (30 nm) reported in most other previous studies on PLLA single crystals.⁷ Earlier studies^{2–7} showed that single crystals of neat PLLA could be obtained only from very dilute solutions (0.05%) or ultrathin film samples (~ 100 nm or less); by contrast, this study has proven that PLLA single crystals of a different morphology could also be prepared from rather concentrated solutions (4 wt %) with a film thickness of 700 nm by controlled phase separation in the PLLA/PBA blend. Note that the concentrations of spin casting and cast film thickness of PLLA/PBA blends are much higher and greater in magnitude than those reported earlier for producing single crystals from neat PLLA.

It is postnoted here that electron diffraction (ED) may ideally yield additional crystal packing information for the lozenge crystals in the melt-crystallized PLLA/PBA (70/30) blend films if suitable samples could be prepared for electron transmission characterization. Other alternative methods were also tried for preparing ED samples: solution cast on silicon wafer and KOH digesting the Si substrate. However, the KOH digestion required a temperature at or higher than 80 °C, which would melt the PLLA/PBA (70/30) blend films and the single crystals therein would exhibit a different pattern from the original morphology. Additionally, thin films were on fine carbon particles (intended for easy removal of cast films) precoated on glass slides; however, the carbon nanoparticles changed the original single crystals and led to a different morphology of tiny spherulites in PLLA/PBA thin films on carbon substrate. ED characterization may be straightforward for solution-grown single crystals, as the solution-grown crystals can be picked up using copper grids. A key contribution of this work was based on an entirely different approach from solution growth or ultrathin nanoconfinement. As a new approach in this study, PLLA single crystals were proven from melt-crystallized and phase-separated PLLA/PBA (70/30) blend intermediate thin films (from 700 nm to nearly 1 μm) on substrates. This submicrometer film thickness would not be thin enough to be suited for TEM and ED patterns, which should be ultrathin ~ 100 nm; in addition, the samples on substrates could not be microtomed from polymer bulks. However, even with the technical difficulty in characterizing its ED patterns, the AFM height and phase imaging results in this study have positively characterized the key features of PLLA single crystals grown in these unusual conditions (blend phase-separation-induced PLLA

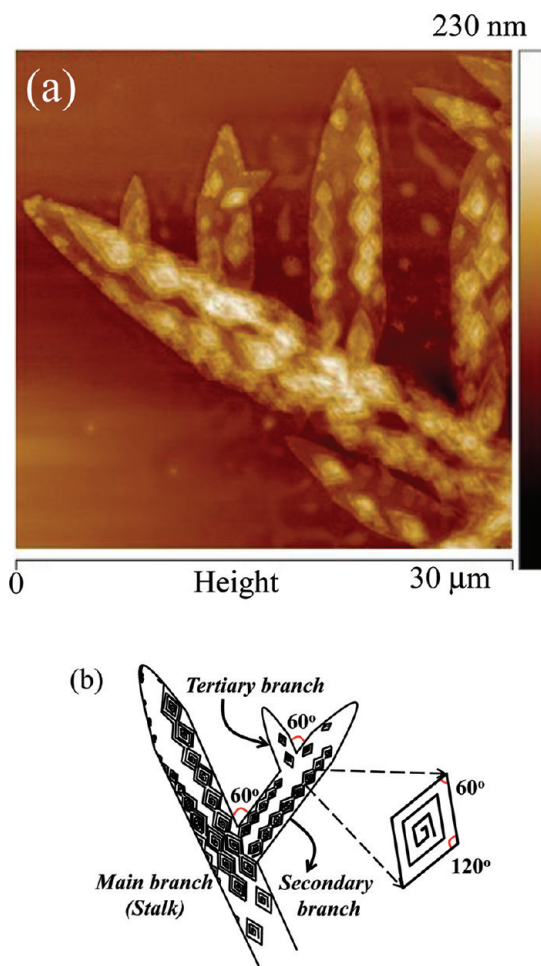


Figure 10. Single crystals in PLLA/PBA (70/30) blend: (a) AFM height image showing single crystals packed into straight dendritic branches; (b) scheme for lozenge-shaped single crystals and their alignment along the branches.

single crystals in meta thin films of submicrometer to 1 μm thickness).

Figure 9 illustrates a scheme for single-crystal layers that are collectively aligned in the dendritic branches, and secondary branches of PLLA crystals in the PLLA/PBA (70/30) crystallized at $T_c = 110^\circ\text{C}$. The second and third layers on the bottom are also built up from spiral growth. However, from the top view and height profile it is very clear that only the top (first) layer shows spiral growth in pyramidal build up; the second and third layers show spiral of sharp-angle turns but on the same height. Three layers of single crystals are common, but they also can be stacked up with more than 3 layers. From the height profiles the total thickness of the three layers is about 56–63 nm. However, the thickness of dendritic single crystals can be as high as ca. 80–90 nm. Thus, there is indication that the main branches may be packed with up to 3 layers of lozenge-shaped crystals, but the secondary side branches are packed only with crystals of 1–2 layers. Short tertiary branches or premature young branches are apparently packed mainly only by one single layer when just initiated.

After proving the lozenge single crystals in the phase-separated PLLA/PBA (70/30) blend, mechanisms of hexastalks and the 60° growth angle of branches in the dendrites can be clearly

interpreted. Figure 10a shows AFM height image of single crystals packed into straight dendritic branches, Figure 10b is scheme for lozenge-shaped single crystals and their alignment along the branches. From Figure 8a it can be seen clearly that lozenge-shaped crystals align along the branch of dendritic PLLA. The dimension of lozenge-shaped crystals is about 0.8–3 μm along the short axis and 1.6–5 μm along the long axis. The size of individual single crystals varies in the stated range. A slanting angle of 60° is clearly visible in branching growth. The angles between growth faces of lozenge-shaped crystal with angular spiraling are about 60° and 120°. This lozenge-shaped geometry in each individual single crystal in melt-crystallized PLLA/PBA (70/30) blend agrees with previous studies reporting single crystals in ultrathin-film neat PLLA.^{3,6}

From the AFM phase images careful inspection reveals that the main stalks of dendrites are composed of about three lines of lozenge-shaped single crystals with each single crystal aligned almost in a straight line and touching each other at the lozenge tips. The ending tips of lozenge crystals likely act as nuclei to nucleate growth of next lozenges in a straight line. The secondary branches, being smaller in transverse diameter, are composed of two lines of lozenge-shaped single crystals with the same alignment and interconnection similar to those in the main hexastalks. The tertiary branches (i.e., branches grown from a secondary branch of dendrites) are usually shorter and thinner and composed of only one or two lozenge-shaped crystals aligned only in one straight line. The six main stalks hexasect the entire dendrites into six equal portions, with a 60° angle between two adjacent main stalks. Due to occasional crystal dislocation at nucleation, twin growth of two main stalks, close and parallel to each, is possible; however, most often the main stalks are individual and widely separated by 60° angle growth. In addition, all main stalks or secondary and tertiary side branches grow exactly with 60° to each other. This 60° growth angle among stalks and branches is identical to the sharp angle (60°) of the lozenge crystal tip. Apparently, the pattern of dendrites is related to the geometry of individual lozenge-shaped crystals, that is, the single crystals are the building blocks for the dendrites with exceptions seen only in occasional crystal dislocations or imperfection.

In summary, AFM observation on individual crystallites reveals that lozenge-shaped single crystals were packed with a clockwise spiral pattern, stacked in layers, and single crystals of 1–3 layers neatly aligned along a straight line. The monolayer thickness of lozenge-shaped single crystals in the top layer was measured to be about 13–34 nm, and the dimension is about 0.8–3 μm along the short axis and 1.6–5 μm along the long axis. Typically, three layers of single crystals are stacked one on another; the lozenge crystals on the bottom layer are about twice as large as those on the top layer, forming a pyramid shape in the depth direction.

Figure 11 shows schemes illustrating three stages of crystal growth and packing of initial single crystals into hexastalk dendrites: (a) individual lenticular-shaped crystals near nuclei, (b) preferential growth along hexasected lines, and (c) final dendrites of hexagon stalks filled with aligned single crystals of lenticular shape. AFM analysis clearly expounded that these lozenge-shaped crystals are aligned hexasected directions into hexastalks dendrites with an occasional side branch, also aligned at 60° to the main branches. Clearly, the hexastalk dendrites observed in the PLLA/PBA (70/30) blend crystallized at $T_c = 110^\circ\text{C}$ are associated with the 60° basal angle of the single crystals at initiation of crystallization near the nuclei center.

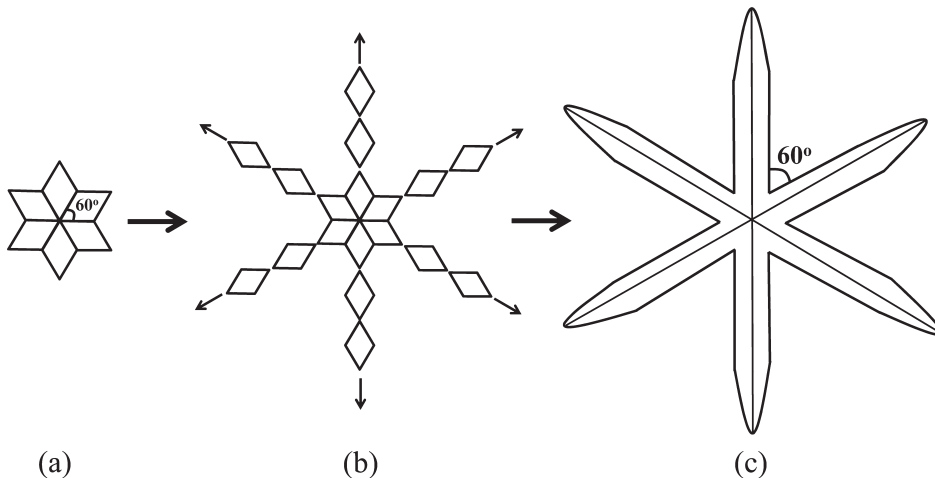


Figure 11. Schemes showing growth and packing of single crystals into hexastalk dendrites in PLLA/PBA (70/30) blend: (a) initial lozenge-shaped crystals near nuclei, (b) growth along hexasected lines, and (c) final dendrites of hexagon stalks with aligned single crystals of lozenge shape.

Interestingly, as the blend compositions were varied by increasing PBA to a higher content, such as 50 wt %, the six-stalk dendrites were no longer present and replaced with PLLA hexagonal crystals near the center and PBA lamellae extending on the peripheral of hexagons (which will be further explored in a future study). This fact indicates that the PLLA single crystals are controlled by exact phase separation into suitable domains in PLLA/PBA (70/30) blend. For other compositions of PLLA/PBA blends lozenge single crystals are not possible. Even for blend compositions near 70/30, such as PLLA/PBA (65/35, 75/25, or any other compositions), the lozenge single crystals or dendrites were not seen.

4. CONCLUSIONS

For the first time, lozenge-shaped single crystals were obtained in PLLA blended with another polyester at a specific composition of PLLA/PBA = 70/30 from melt-crystallized ($T_c = 110^\circ\text{C}$) films at a not-so-thin (intermediate) thickness of 700 nm. Melt crystallization of other PLLA/PBA blend compositions or at another T_c led to different morphologies far away from the lozenge single crystals. Correlations with phase separation and mechanisms of hexastalk-grown dendrites using the lozenge-shaped crystals as building blocks were also new. A phase-separation-induced single-crystalline morphology took place only in a specific composition of PLLA/PBA blend (70/30) of thickness = 700 nm upon melt crystallization at $T_c = 110^\circ\text{C}$. In the PLLA/PBA (70/30) blend, melt crystallization in thin films of 700 nm thickness is shown to pack into single crystals of lozenge shapes and 1–3 layers with an apparently clockwise spiral pattern in the top layer. The dendritic branches of the single crystal were analyzed to pack by aligning into hexastalk dendrites with occasional side branches (secondary or tertiary). The individual single crystals had lozenge shapes of 1.6–5 μm in the long axis or 0.8–3 μm in the short axis, as revealed clearly in the AFM images. The monolayer thickness of the melt-crystallized lozenge-shaped single crystals in the PLLA/PBA blend is about 13–34 nm, which is comparable to the dimensions of solution-grown single crystals. All branches from the PLLA hexastalk dendrites grow exactly in 60° direction to each other, and this growth angle coincides with the tip angle of the lozenge-shaped single crystals, indicating that growth of the stalks and all

branches in the dendrites is governed by geometry confinement of the single crystals. The mechanism of crystal growth along the 60° angle is a result of the basal angle of the single crystals at initiation of crystallization near the nuclei center.

In the PLLA/PBA blends with PBA contents of 10, 20, and 25 wt % there is no phase separation in these blend systems; consequently, no single-crystalline morphology is present in these blend compositions. Apparently, phase separation induces formation of PLLA single crystals in PLLA/PBA (70/30) blend. All PBA are rejected from the growth front of PLLA at $T_c = 110^\circ\text{C}$ and crystallized at ambient temperature as ring-banded spherulites inside of discrete domains only, resulting in a favorable environment for formation of PLLA single crystals.

■ AUTHOR INFORMATION

Corresponding Author

*Phone: +886 6 275-7575 ext. 62670. Fax: +886 6 234-4496. E-mail: emwoo@mail.ncku.edu.tw.

■ ACKNOWLEDGMENT

This work was financially supported by a basic research grant (NSC-97-2221-E-006-034-MY3 and NSC 99-2221-E-006-014-MY3) for three consecutive years from Taiwan's National Science Council (NSC) to which the authors express their gratitude.

■ REFERENCES

- (1) Kalb, B.; Penning, A. J. *Polymer* **1980**, *21*, 607–612.
- (2) Miyata, T.; Masuko, T. *Polymer* **1997**, *38* (16), 4003–4009.
- (3) Iwata, T.; Doi, Y. *Macromolecules* **1998**, *31*, 2461–2467.
- (4) Lee, W.-K.; Lee, J.-K.; Ha, C.-S. *Macromol. Res.* **2003**, *11* (6), 511–513.
- (5) Fujita, M.; Doi, Y. *Macromolecules* **2003**, *4*, 1301–1307.
- (6) Lee, W.-K.; Iwata, T. *Ultramicroscopy* **2008**, *108*, 1054–1057.
- (7) Maillard, D.; Prud'homme, R. E. *Can. J. Chem.* **2008**, *86*, 556–563.
- (8) Kikkawa, Y.; Abe, H.; Iwata, T.; Inoue, Y.; Doi, Y. *Biomacromolecules* **2002**, *3*, 350–356.
- (9) Su, F.; Iwata, T.; Sudesh, K.; Doi, Y. *Polymer* **2001**, *42*, 8915–8918.
- (10) Iwata, T.; Doi, Y. *Polym. Int.* **2002**, *51*, 852–858.
- (11) Núñez, E.; Gedde, U. W. *Polymer* **2005**, *46*, 5992–6000.
- (12) Sun, J.; Chen, X.; He, C.; Jing, X. *Macromolecules* **2006**, *39*, 3717–3719.

- (13) Iwata, T.; Doi, Y.; Isono, K.; Yoshida, Y. *Macromolecules* **2001**, *34*, 7343–7348.
- (14) Alemán, C.; Lotz, B.; Puiggali, J. *Macromolecules* **2001**, *34*, 4795–4801.
- (15) Zhang, J. M.; Duan, Y.; Sato, H.; Tsuji, H.; Noda, I.; Yan, S.; Ozaki, Y. *Macromolecules* **2005**, *38*, 8012–8021.
- (16) Chiang, Y.-W.; Ho, R.-M.; Thomas, E. L.; Burger, C.; Hsiao, B. S. *Adv. Funct. Mater.* **2009**, *19*, 448–459.
- (17) Yang, J.; Zhao, T.; Zhou, Y.; Liu, L.; Li, G.; Zhou, E.; Chen, X. *Macromolecules* **2007**, *40*, 2791–2797.
- (18) Huang, S.; Jiang, S.; An, L.; Chen, X. *J. Polym. Sci., Part B: Polym. Phys.* **2008**, *46*, 1400–1411.
- (19) Huang, S.; Jiang, S.; Chen, X.; An, L. *Langmuir* **2009**, *25* (22), 13125–13132.
- (20) Horn, R. M. V. Dissertation: Tethered Polymer Chains On Single Crystal Surfaces; The Graduate Faculty of The University of Akron: Akron, OH, Aug 2009.
- (21) Xiong, H.; Zheng, J. X.; Horn, R. M. V.; Jeong, K.-U.; Quirk, R. P.; Lotz, B.; Thomas, E. L.; Brittain, W. J.; Cheng, S. Z. D. *Polymer* **2007**, *48*, 3732–3738.
- (22) Hsiao, M.-S.; Zheng, J. X.; Leng, S.; Horn, R. M. V.; Quirk, R. P.; Thomas, E. L.; Chen, H.-L.; Hsiao, B. S.; Rong, L.; Lotz, B.; Cheng, S. Z. D. *Macromolecules* **2008**, *41*, 8114–8123.
- (23) Snétivy, D.; Vancso, G. J. *Polymer* **1992**, *33*, 432–433.
- (24) Huang, I.-H.; Chang, L.; Woo, E. M. *Macromol. Chem. Phys.* **2011**, *212*, 1155–1164.
- (25) Lee, S.-H.; Jhon, M. S.; Eyring, H. *Proc. Natl. Acad. Sci. U.S.A.* **1977**, *74*, 10–12.
- (26) Robeson, L. M. *Polymer Blends: A Comprehensive Review*; Hanser: Munich, 2007.